DENTAL MATERIALS 35 (2019) 636–649

Available online at www.sciencedirect.com

ScienceDirect

journal homepage: www.intl.elsevierhealth.com/journals/dema

An integrated multifunctional hybrid cement (pRMGIC) for dental applications

Lamis Al Taee[a], *Avijit Banerjee*[b], *Sanjukta Deb*[a,*]

[a] *Centre for Oral, Clinical & Translation Sciences, Faculty of Dentistry, Oral & Craniofacial Sciences, Floor 17, Tower Wing, Guy's Hospital, London Bridge, London, SE1 9RT, UK*

[b] *Conservative & MI Dentistry, Centre for Oral, Clinical & Translation Sciences, Faculty of Dentistry, Oral & Craniofacial Sciences, Floor 26, Tower Wing, Guy's Hospital, Great Maze Pond, London, SE1 9RT, UK*

ARTICLE INFO

Article history:
Received 23 August 2018
Accepted 7 February 2019

Keywords:
Ethylene glycol methacrylate phosphate
Resin modified glass ionomer cements
Adhesive dental cements
Dental reparative biomaterial
Minimally invasive dentistry

ABSTRACT

Objective. Glass-ionomer and resin-modified glass-ionomer cements are versatile materials with the ability to form a direct bond with tooth tissues. The aim of this study was to formulate a novel class of dental bio-interactive restorative material (pRMGIC) based on resin-modified glass-ionomer cements via the inclusion of an organophosphorus monomer, ethylene glycol methacrylate phosphate, with a potential to improve the mechanical properties and also function as a reparative restorative material.

Methods. pRMGIC was formulated with modification of the resin phase by forming mixes of ethylene glycol methacrylate phosphate (EGMP; 0–40%wt) and 2-hydroxyethyl methacrylate monomer into the liquid phase of a RMGIC (Fuji II LC, GC Corp.). The physical properties of the cements were determined including setting characteristics, compressive strength and modulus (CS &CM), microhardness (MH) and biaxial flexural strength (BFS). Fluid uptake and fluoride release were assessed up to 60 days storage. Adhesion to sound dentine was measured using micro-tensile bond strength and surface integrity was analysed using SEM coupled with EDX. Statistical analysis was performed using ANOVA and Bonferroni post-hoc tests.

Results. The pRMGIC cements exhibited an increase in working time with increasing EGMP concentration however were within the limits of standard clinical requirements. Although the compressive strength of pRMGIC cements were comparable to control cements in the early stages of maturation, the higher EGMP-containing cements (EGMP30 and 40) exhibited significantly greater values ($p < 0.05$) after 4 weeks storage (141.0 ± 9 and 140.4 ± 8 MPa, respectively), in comparison to EGMP0 (128.8 ± 7 MPa). A dramatic two fold increase in biaxial flexural strength ($p < 0.001$) was observed for the pRMGIC's. Furthermore, the ability to decalcify tooth apatite resulted in enhanced interfacial adhesion due to chelation with calcium ions of tooth apatite. The inclusion of EGMP encouraged formation of reinforcing complexes within the RMGIC, thus improving physical properties, decreasing solubility and lower fluoride release. A dense microstructure was observed with increasing EGMP content.

Significance. A novel universal bio-interactive adhesive repair material will enable clinicians to offer more effective repair of the tooth-restoration complex, thus future treatments will benefit both patient and a severely constrained healthcare budget.

* *Corresponding author.*
E-mail address: sanjukta.deb@kcl.ac.uk (S. Deb).

https://doi.org/10.1016/j.dental.2019.02.005

1. Introduction

Tooth decay (dental caries) is a bacterially-mediated, non-communicable disease (NCD), which is recognized as the primary cause of oral pain and tooth loss in all age groups globally [1–3]. According to the World Health Organisation (WHO), this is the most prevalent of preventable, lifestyle-related NCDs affecting humankind, which still presents a major global health burden especially because of its profound effect on general health and well-being, as well as being associated both directly and indirectly with other systemic, chronic conditions [4]. The treatment of its adverse dental effects, cavities in teeth, involves the surgical excision of necrotic tooth tissue followed by restoration of the cavity with artificial dental biomaterials, i.e. fillings/restorations, by the dental practitioner. There are a number of dental restorative materials which provide adequate function and aesthetics, however maintaining the long term functional integrity of the tooth-restoration complex (TRC) still remains a challenge in clinical operative dentistry. The contemporary minimally invasive management approach helps increase TRC longevity [5]. Tooth-restoration complex failures may occur either in the restorative material or the tooth itself, or both. Restorations are likely to fail mechanically, such as bulk fracture, staining, loss of retention and deficient marginal adaptation [6,7]. In contrast, tooth failures are correlated to mechanical, structural and biological reasons (caries associated with restorations and sealants {CARS} and fractured cusps) [1,5]. These failures may occur independently or combined in addition to clinician/patient-related factors [8]. In addition, a significant proportion of dental health service budgets are dedicated to the replacement of restorations, which have a limited lifespan. Hence lowering the burden of replacing failed restorations through minimally invasive approaches is of importance because with each intervention, the likelihood of unnecessary tooth tissue loss increases [5,9,10]. Repair helps limit the traditional, complex and more destructive restorative therapy involved in replacing restorations and reduces treatment costs whilst allows preservation of tooth structure and consequently increases the longevity TRCs [9–11]. However, there are no dedicated reparative dental biomaterials and the use of existing materials often result in inadequate clinical outcomes [10].

Utilising the inherent ability of resin-modified glass-ionomer cements (RMGICs) [12] to adhere to tooth tissue [13], the incorporation of a polymerisable phosphate-based monomer, namely ethylene glycol methacrylate phosphate (EGMP), by immobilizing it in the cement, promotes the interaction of the ligating phosphate groups with the ions within the glass matrix and mineral component of tooth tissue. In addition, these polar phosphate groups tethered to the polymer backbone may enable higher affinity and bonding efficacy to relevant substrates. The EGMP-HEMA allows for the polymerisation, which is hypothesized to not only create a network of covalently-linked phosphate groups, but additionally improve adhesion to dental resin composites, RMGIC/GIC's and amalgams by virtue of the polar phosphate groups. EGMP is a proton-conducting electrolyte and the complexation behaviour of the carbonyl and phosphoryl

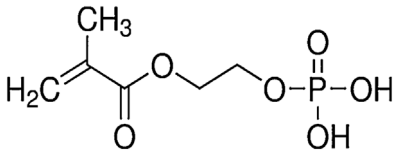

Fig. 1 – Chemical structure of ethylene glycol methacrylate phosphate.

ligating groups has been reported to enable remineralisation in hydrogels [14] due to the charge in the gel and also improves the bonding efficacy and durability of self-etching adhesives [15–18]. This study reports the setting kinetics, mechanical properties (compressive strength and modulus, microhardness and biaxial flexural strength), fluid uptake, fluoride release of the pRMGIC's and investigates the efficacy of the modified cement to be used for repairing failed TRCs. The hypothesis tested was that the incorporation of different proportions of EGMP (1 0-40% wt.) into a commercial RMGIC have no significant effect on their physical and bonding properties, and subsequent ageing has no bearing on the properties of the modified formulations.

2. Materials and methods

2.1. *Materials*

Ethylene glycol methacrylate phosphate was purchased from Polysciences Europe GmbH, Germany (Batch No.: 52628-03-2, molecular weight 210.12 g/mol, density1.37 g/mL). The chemical structure is shown in Fig. 1. Commercial RMGIC Fuji II LC (Improved), shade A2 (batch numbers 141118, and 1412081, GC Corp., Europe) was used as a control. It consists of a calcium fluoroaluminosilicate glass and an aqueous solution containing 25–50% 2-hydroxyethyl methacrylate (HEMA), 5–10% polyacrylic acid, and 1–5% urethane dimethacrylate (UDMA), initiators and pigments.

2.2. *Formulation and characterization of the pRMGIC*

2.2.1. *Specimen preparation*

The new cement was formulated by incorporating different proportions of EGMP monomer (10, 20, 30 and 40% by weight) into the liquid phase of commercial Fuji II LC. The powder component of the RMGIC was used without any modification in all cement formulations. The unaltered Fuji II LC cement was used as a control (EGMP0), whereas the experimental groups were prepared by hand-mixing of the commercial Fuji II LC glass powder with the modified liquid (EGMP10, EGMP20, EGMP30, and EGMP40) using a powder/liquid ratio 3.2/1.0, at ambient temperature ($23 \pm 2\,^{\circ}C$) and humidity ($35 \pm 5\%$). The cement formulations with their respective codes are shown in Table 1. The freshly mixed cement pastes were placed in cylindrical polyethene split moulds (4 mm diameter, 6 mm height) to prepare test specimens for determining compressive strength (CS) and microhardness (MH) (ISO, 9917-2, 2010 water-based dental cements) [19]. A stainless-steel mould of 8.3 mm diameter and 1.3 mm thickness was used to prepare the disc specimens for the biaxial flexural strength (BFS) test.

Table 1 – Composition of the control and experimental pRMGIC cements.

Codes/liquid phase	Solid phase	EGMP (wt %)	P/L ratios
EGMP0 (Fuji II LC liquid)	GC Fuji II LC powder	0 (control)	3.2/1.0
EGMP10	GC Fuji II LC powder	10	3.2/1.0
EGMP20	GC Fuji II LC powder	20	3.2/1.0
EGMP30	GC Fuji II LC powder	30	3.2/1.0
EGMP40	GC Fuji II LC powder	40	3.2/1.0

Specimens were photo-polymerised using a light curing device (Elipar™ DeepCure-S LED, 3M USA) with a light intensity of 1470 mW/cm^2 for 30 s at each end of the cylindrical mold, and 20 s on the top surface of disc specimens. The CS, MH and BFS tests were carried out after 1, 14, 28 and 180 days storage in simulated body fluid (SBF) at 37 °C. Water uptake behaviour and fluoride release were assessed in accordance to ISO guidelines (ISO 4049. Dentistry-resin based dental fillings. ISO; 2009) [20].

2.2.2. *Curing parameters*

The working and setting times of the cements were determined using an oscillating rheometer (Sabri Dental Enterprises, 1404 Brook drive, USA) at ambient temperature. A powder/liquid ratio of 3.2/1.0 were used for preparation of the cements. Measurements were made in triplicate.

2.2.3. *Spectral analysis by Fourier transform-infrared spectroscopy (FTIR)*

ATR/FTIR vibrational analysis (IR) was performed using a Perkin Elmer Spectrum One FTIR Spectrometer (Perkin-Elmer, Beaconsfield, UK) with a resolution of 4 cm^{-1}. The infrared spectra were recorded in the spectral range of 4000–600 cm^{-1}, with eight scans each.

2.2.4. *Mechanical properties*

320 cylindrical specimens (n = 8 per each group) were prepared for CS and MH tests; these properties were tested after 1, 14, 28 and 180 days ageing in SBF. The surface microhardness was determined using a Knoop hardness testing machine (Duramin10, Struers, Japan) with 50 g load for 10 s at 6 randomly selected areas on each of the 8 specimens. A universal testing machine (Instron model 5569, USA) with a 500 N load cell was used for testing the compressive strength and modulus at a crosshead speed of 0.5 mm/min. For the BFS test, the specimens (n = 32 per group) were placed on a 6.5 mm diameter circular support. A universal testing machine (Instron Model 5569, USA) at a crosshead speed of 0.5 mm/min, was used to load the specimens centrally through a rounded tip indenter, in a way that the area of maximum tensile stress was located at the centre of the lower face of the disc. The BFS values were calculated using the following Eqs. (1)–(3): [21]

$$\sigma = \frac{AP}{t^2} \tag{1}$$

$$A = 3/(4\pi)[2\,(1+\upsilon)\,\ln(a/r_0^*) + (1-\upsilon)\{\frac{2a^2 - r_0^{*2}}{2b^2}\} + 1 + \upsilon] \tag{2}$$

where P is the applied load at failure, υ is Poisson's ratio (0.35) [21], a is the radius of support circle, b is the radius of disc specimen, t is the thickness of the disc specimen, and r_0 is the radius of the ball used on the loading surface:

$$r_0^* \sqrt{\left(1.6r_0^2 + t^2\right) - 0.675t} \tag{3}$$

where r_0 is an equivalent radius of contact between the loading ball and the disc specimen, where loading can be considered uniform.

2.2.5. *Mass change during water uptake*

Disc-shaped specimens were made using moulds (10 mm diameter,1 mm thickness) at (23 ± 1)°C, following ISO standard 4949:2009 [20]. The dimensions were recorded and mean values were used to calculate the volume of each specimen in mm^3. (Mettler Toledo XS105DU, Switzerland) to an accuracy of ±0.0001 g. Specimens were immersed in 10 ml distilled water at 37 °C individually for a total immersion time of 60 days. At defined time intervals, the specimens' surfaces were blotted gently with filter paper and weighed. Several readings (w_t) were taken on the first day, daily for a week, then weekly thereafter until equilibrium was achieved, indicated by four successive measurements being the same. The mass recorded at equilibrium was denoted as (w_e).

$$\textit{Weight change}\,(\%) = \frac{w_t - w_0}{w_0} \times 100 \tag{4}$$

where w_t, weight at t time, w_0, initial weight of the specimen. The mean weight change (%) and standard deviation (SD) during water uptake were plotted against time$^{1/2}$(seconds) to create the weight change profile for each tested group. After equilibrium, the specimens were desorbed at 37 °C to obtain water loss, until reaching a constant weight (w_d). The water sorption (WSP) in μg/mm^3 at the equilibrium stage was calculated using the equation:

$$WSP = w_e - w_d/V \tag{5}$$

w_e weight at the equilibrium after uptake, w_d the constant weight after desorption, V volume [22]. The solubility percentage was calculated by subtracting the weight after desorption (w_d) from the initial specimen weight (w_0), Eq. (6). This is equivalent to the total mass of components leached from the material.

$$\textit{Solubility}\,(\%) = \left(\frac{W_0 - W_d}{W_0}\right) \times 100 \tag{6}$$

W_0 initial weight, W_d weight at the equilibrium after desorption.

The solubility (WSL) in $\mu g/mm^3$ calculated using the following Eq. (7):

$$WSL = W_0 - W_d/V \quad (7)$$

W_0 initial weight, W_d weight at the equilibrium after desorption, V volume.

The water uptake data were plotted as Mt/M∞ against time$^{1/2}$ (seconds$^{1/2}$) to obtain the slope used to calculate the diffusion coefficient for the water uptake process, using Eq. (8), [22]

$$D = \frac{s^2 \pi l^2}{4} \quad (8)$$

where s = slope of graph; Mt = the mass uptake/loss at time t (s); M∞ = equilibrium uptake/loss, l = the thickness of the specimens, and D is the diffusion coefficient.

2.2.6. *Fluoride release*

Fluoride ion release measurements were recorded 60 days (n = 5 per each group) using disc-shaped specimens (8.3 mm diameter × 1.3 mm thickness). Each specimen was immersed in an individually capped polystyrene tube containing 2 ml of distilled water (pH 7.0) and stored at 37 °C for a total immersion time of 60 days. The storage medium was refreshed to avoid fluoride saturation of the solution, and fluoride concentration measured at different intervals. An equal volume (2 ml) of total ionic strength adjustment buffer (TISAB I BDH Ltd., Poole, England) was added prior to fluoride ion measurements, which increases the ionic strength of the solution to a relatively high level and hence increases the accuracy of the reading. Fluoride concentrations were recorded in ppm using a selective fluoride electrode (Cole Parmer 27502) connected to an ion analyzer (OAKTON 510 ion series, Singapore). The amount of fluoride eluted from the cements was converted into milligrams of F-released per unit surface of area (mg F/cm^2).

2.2.7. *Adhesion to sound dentine*

The bonding efficacy of the RMGICs (experimental and control) to sound dentine was evaluated using microtensile bond strength tests (μTBS) and scanning electron microscopy (SEM) used to assess the mode of failure of the debonded interfaces. Ten permanent sound molars were collected using an ethics protocol reviewed and approved by NHS health research authority (16/SW/0220). The occlusal enamel was removed using a low-speed water-cooled diamond saw microtome (Isomet 1000, Buehler, Lake Bluff, IL, USA). The dentine surface was polished for 60 s using 600 grit polishing paper followed by the application of dentine conditioner (10% polyacrylic acid, GC Corp) for 20 s to remove any smear layer. The conditioner was washed with air/water spray for 15 s and dried with a gentle stream of dry compressed air for 15 s. A matrix band was secured around each specimen, and the RMGICs (control and experimental groups) were placed over the dentine surfaces and photo-polymerized for 40 s using a light curing device (Elipar™ DeepCure-S LED, 3M USA) with a light intensity of 1470 mW/cm^2. The restored specimens were stored at 37 °C and 100% humidity for 24 h before sectioning. Individual beams were sectioned occluso-gingivally to produce 0.9 mm × 0.9 mm specimens, with the RMGICs comprising the upper half of the beam and dentine comprising the lower half. Twenty beams per group were stored for two weeks in SBF at 37 °C. Specimens were stressed to failure under tension using a universal testing machine (SMAC Europe Ltd, Crawley, UK) at a crosshead speed of 0.5 mm per min. The failure modes of the bonds were initially evaluated at x40 with a stereoscopic microscope. Failures were classified as interfacial failure between dentine and the RMGIC, cohesive failure within the RMGIC/ or dentine, and mixed (combinations of cohesive failure in the RMGIC/dentine and interfacial failure along the dentine surface).

2.2.8. *Scanning electron microscopy and energy dispersion X-ray spectroscopy*

Representative surfaces from mechanical testing (CS and BFS) were dried, carbon-coated, and viewed using scanning electron microscopy (JCM-6000 PLUS, NeoScope - Benchtop SEM, USA) with an accelerating voltage of 10 kV. Scanning electron micrographs of the fractured specimens from CS test showed the microstructural changes for selected cement formulations (EGMP0, EGMP20, and EGMP30) at different magnifications (×50, ×100 and ×400). Scanning electron micrographs at ×50, ×600, and ×1000 magnification were also performed to assess the surface morphology of the fractured specimens from BFS test for all formulations after four weeks' storage in SBF at 37 °C. These were coupled to an energy dispersive X-ray spectroscope (EDX) (JCM-6000 PLUS, JED-2300 Analysis Station Plus, USA) to perform elemental analysis for all tested cements. For the μTBS test, SEM of representative debonded specimens of the EGMP0 and EGMP30 only (n = 2 per group) which showed mixed or adhesive failures were obtained. Specimens were dried and gold coated at 45 mA currents for 2 min and viewed under a SEM (JCM-6000 PLUS, NeoScope - Benchtop SEM, USA) at magnification power ×100, and ×1000.

2.3. *Statistical analysis*

Data were tested for normality using Q–Q plots and Shapiro–Wilk tests and were analyzed parametrically as the data followed a normal distribution. One-way analysis of variance (ANOVA) and Bonferroni HSD post hoc tests were employed to calculate significance (alpha level = 0.05) in mean values amongst the tested groups at each time interval. Independent t-tests ($p < 0.05$) was also applied to determine the effects of different storage time on the mechanical properties per each group. All analyses were conducted using SPSS statistical package (version 24; SPSS® Inc., IBM®, Chicago, IL, USA).

3. Results

3.1. *Setting parameter of the cements*

The curing parameters of the cements is shown in Table 2. At lower concentrations of EGMP, no discernible changes were observed in the working time of the cements. A statistically significant increase in working time ($p < 0.05$) resulted at higher concentrations of 30-40 wt% EGMP in the formu-

Table 2 – The working and setting time of the experimental cements with GC Fuji II LC powder and liquid phase with different concentrations of EGMP at a powder: liquid ratio of 3.2:1. (*) denotes a statistically significant difference at $p < 0.05$.

Groups/n = 3	Working time (min)	Setting time (min)
EGMP0	3.45 (0.2)	5.33 (0.1)
EGMP10	3.44 (0.1)	5.40 (0.2)
EGMP20	3.46 (0.2)	5.43 (0.2)
EGMP30	4.24 (0.1)*	5.63 (0.2)
EGMP40	4.00 (0.1)*	5.60 (0.2)

* Significant difference of the experimental RMGICs from the control group (Bonferroni test post-hoc tests, alpha level of 0.05).

lations (4.2 and 4 min, respectively) as compared to Fuji II LC (3.45 min), however they were within acceptable limits as stipulated by ISO standards and met the requirements for water-based cements. The setting time of all formulations were comparable to the control cement and remained unaffected on inclusion of EGMP at the concentrations studied.

3.2. FTIR

The FTIR spectrum of the pRMGIC cements and control RMGIC after 4 weeks immersion in SBF is shown in Fig. 2. The FTIR spectra showed a broad medium absorption band at 1719 cm^{-1} assigned to the carbonyl stretching vibration of the ester groups. The characteristic peaks of the polyacrylate salt formation were evident with symmetric and asymmetric —COO stretching bands at approximately 1450 and 1580 cm^{-1} confirming the occurrence of the acid-base reaction. Changes were observed in the intensity of the peak arising at 1024 cm^{-1}, with evidence of a new shoulder peak at approximately 966 cm^{-1}, which increased in intensity with increasing EGMP content within the matrix. This was assigned to $\nu 3$ and $\nu 1$ stretching vibrations of the phosphate tetrahedral structure as shown in the FTIR spectra in Fig. 2.

3.3. Mechanical properties

The mechanical properties of the cements are presented in Table 3. The compressive strengths of the pRMGICs (EGMP10, 30 and 40) at 24 h were similar to the control. After 14 days of storage in SBF at 37 °C, all groups exhibited an enhanced CS in comparison to their early storage values ($p < 0.05$) but with no statistically significant differences amongst them. The higher EGMP-containing cements (EGMP30 and 40) continued gaining strength after 4 weeks ageing (141.0 ± 9 and 140.4 ± 8 MPa, respectively) and were significantly higher than the control cement (128.8 ± 7 MPa) ($p < 0.05$). On longer term ageing (180 days), the CS deteriorated for the control cements but was maintained in all modified formulations with statistically significant differences from the commercial reference and their initial values ($p < 0.05$).

The pRMGIC cements exhibited a significant enhancement in the compressive modulus in comparison to the control cement at most time points ($p < 0.05$). The values increased proportionally with higher EGMP content. Prolonged ageing in SBF raised the CM of the EGMP20, 30, and 40 cements

Table 3 – Compressive strength (CS) and modulus (CM), microhardness (MH) and biaxial flexural strength (BFS) of the pRMGICs (0–40%) at 1, 14, 28 and 180 days aged in SBF at 37°C, shown as mean (SD), n = 8.

Days	EGMP0	EGMP10	EGMP20	EGMP30	EGMP40
	CS (MPa)	CS (MPa)	CS (MPa)	CS (MPa)	CS (MPa)
1	108.3 (6.5)[a]	102.9 (8.4)[a]	119.6 (7.4)*,[b]	117.3 (7.3)[ab]	116.7 (7.4)[ab]
14	131.0 (7.6)[c,^]	132.7 (7.9)[c,^]	131.8 (7.8)[c,^]	138.9 (9.5)[c,^]	131.6 (6.0)[c,^]
28	128.8 (7.5)[d,^]	131.4 (7.1)[de,^]	132.9 (6.6)[de,^]	141.0 (8.8)*,[e,^]	140.4 (8.0)*,[e,^]
180	107.8 (7.8)	121.9 (8.4)*,[f,^]	131.5 (8.0)*,[fg,^]	138.9 (8.4)*,[g,^]	121.3 (7.1)*,[f]
	CM (GPa)	CM (GPa)	CM (GPa)	CM (GPa)	CM (GPa)
1	2.4 (0.4)	3.2 (0.3)*,[a]	3.4 (0.3)*,[ab]	3.8 (0.3)*,[bc]	3.9 (0.3)*,[c]
14	3.1 (0.3)[^]	4.0 (0.3)*,[d,^]	4.3 (0.4)*,[de,^]	4.5 (0.2)*,[ef]	4.9 (0.3)*,[f,^]
28	2.8 (0.3)	3.7 (0.4)*,[g]	3.8 (0.4)*,[gh]	4.2 (0.5)*,[gh]	4.4 (0.3)*,[h]
180	3.0 (0.3)[I,^]	3.6 (0.6)[ij]	4.2 (0.4)*,[jk,^]	4.5 (0.3)*,[k,^]	4.5 (0.4)*,[k,^]
	MH (KHN)	MH (KHN)	MH (KHN)	MH (KHN)	MH (KHN)
1	31.7 (1.8)[a]	33.0 (1.3)[a]	35.8 (3.0)[ab]	38.3 (3.1)*,[bc]	39.9 (3.9)*,[b]
14	32.0 (1.9)	39.6 (2.9)*,[^]	43.3 (1.7)*,[^]	48.8 (2.0)*,[d,^]	46.8 (2.3)*,[d,^]
28	29.7 (3.3)	42.1 (2.9)*,[e,^]	45.1 (3.4)*,[ef,^]	49.0 (2.7)*,[f,^]	45.9 (3.6)*,[ef,^]
180	31.5 (2.8)	36.4 (3.3)*,[f,^]	39.2 (3.5)*,[fg]	46.6 (2.7)*,[^]	45.0 (2.8)*,[g]
	BFS (MPa)	BFS (MPa)	BFS (MPa)	BFS (MPa)	BFS (MPa)
1	121.8 (7.3)	249.2 (15.7)*,[a]	282.7 (15.2)*	228.2 (14.6)*,[a]	200.9 (14.9)*
14	143.6 (16.6)[^]	291.7 (15.7)*,[b,^]	290.6 (17.8)*,[b]	265.6 (20.2)*,[b,^]	219.1 (15.7)*
28	94.6 (8.6)[^]	241.1 (11.7)*,[c]	269.0 (16.4)*,[d]	254.2 (11.3)*,[cd,^]	246.0 (13.9)*,[cd,^]
180	133.6 (12.1)	231.6 (11.5)*,[e]	251.4 (13.1)*,[f,^]	253.8 (9.5)*,[f,^]	237.2 (11.6)*,[ef,^]

Similar letters in rows indicate no significant differences among groups (ANOVA, Bonferroni test post-hoc tests, alpha level 0.05).
* Significant difference between pRMGICs and control group.
^ Significant effect of ageing for the same group from day1 values within each column.

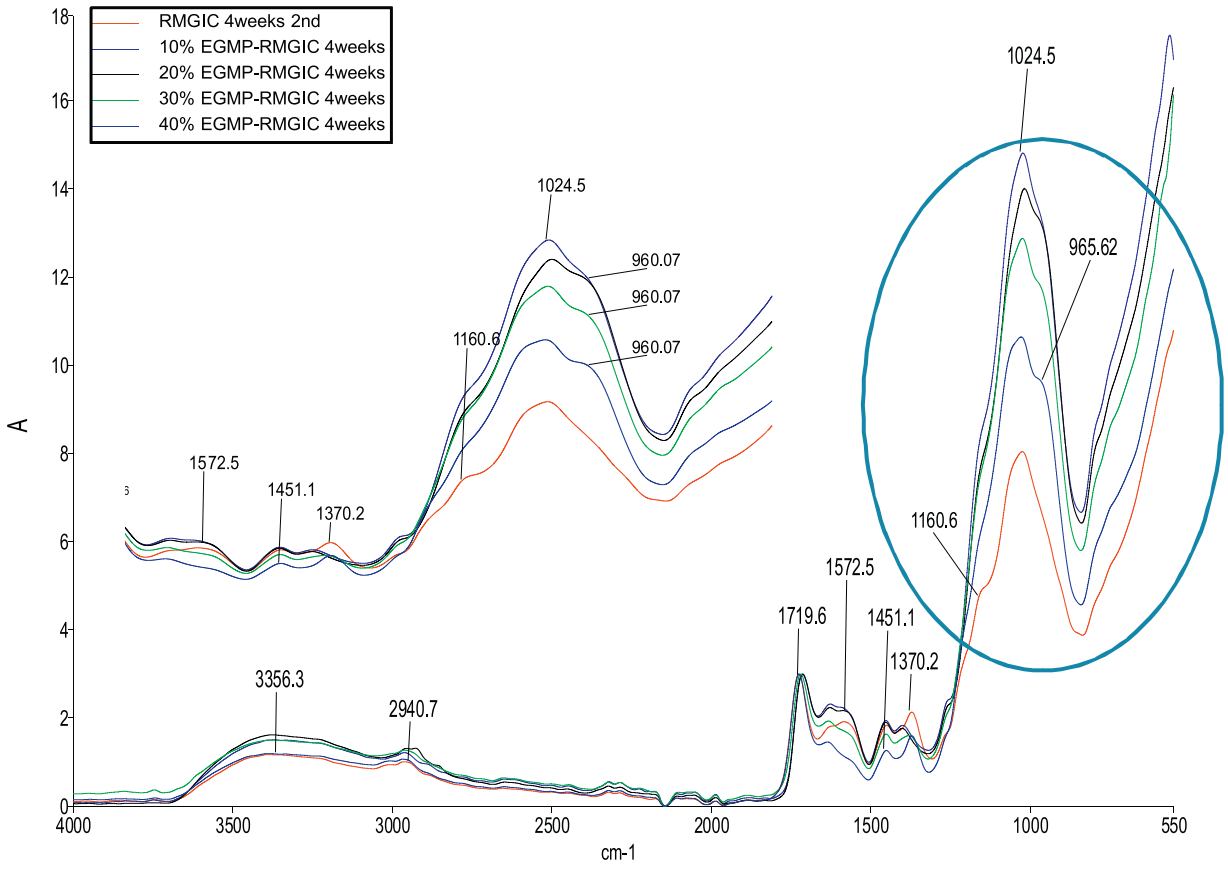

Fig. 2 – A comparison of the FTIR spectra of the control RMGIC and the experimental cements pRMGIC's after 4 weeks interaction with water.

as compared to the control group and their corresponding immediate values ($p < 0.05$). The microhardness of the pRMGIC cements were higher for the EGMP30 & EGMP40 cements, however on storage, all the pRMGIC cements showed statistically significantly higher values from the control up to 6 months ($p < 0.05$). The profound effect of EGMP was evident in the biaxial flexural strength, which showed a two-fold increase in values ($p < 0.001$) in comparison to the control at all time intervals. Ageing showed a variable effect on the values among experimental groups, but EGMP20 and 30 maintained high flexural strength up to 6 months storage (Table 3).

3.4. *Interaction with water*

The pRMGIC cements exhibited higher percentage water uptake as compared to the control (EGMP0), which increased proportionally with increasing EGMP content within the matrix, Table 4, whilst all cements attained equilibrium uptake within a week. The water uptake values ranged from 56.7–60.7 $\mu g/mm^3$ for the pRMGIC cements with 54.7 $\mu g/mm^3$ for the control cement.

The solubility (percentages and in $\mu g/mm^3$) was significantly lower in pRMGIC in comparison to the control cement (EGMP0) ($p < 0.001$) as shown in Table 4. The values

Table 4 – Water uptake of the commercial and experimental pRMGICs for a total immersion time of 60 days in distilled water 37°C (n = 5). (*) significant difference one-way ANOVA with Bonferroni post-hoc test, alpha level of 0.05.

Days	Equilibrium water uptake		Solubility		Diffusion coefficient
	%	μgmm^3	%	μgmm^3	$(10^{-11}\ m^2 s^{-1})$
EGMP0	7.9 (0.3)	54.7 (2.0)	1.5 (0.10)	9.6 (0.3)	2.29
EGMP10	8.8 (0.3)	56.7 (2.0)	0.6 (0.02)*	3.3 (0.1)*	2.04
EGMP20	9.4 (0.3)*	57.5 (1.6)	0.4 (0.05)*	2.5 (0.1)*	1.89
EGMP30	10.1 (0.4)*	58.5 (1.9)	0.4 (0.06)*	2.2 (0.1)*	1.52
EGMP40	10.1 (0.4)*	60.7 (1.3)*	0.3 (0.04)*	2.2 (0.1)*	1.02

* Significant difference of the experimental RMGICs from the control group. One-way ANOVA with Bonferroni post-hoc test, an alpha level of 0.05.

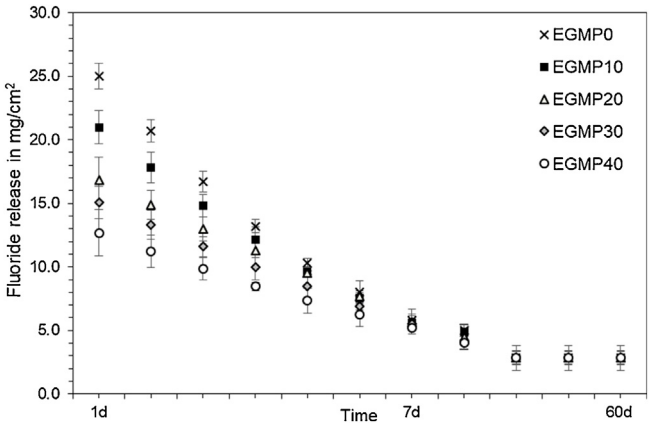

Fig. 3 – Fluoride release in mg/cm² for control and experimental pRMGICs over time.

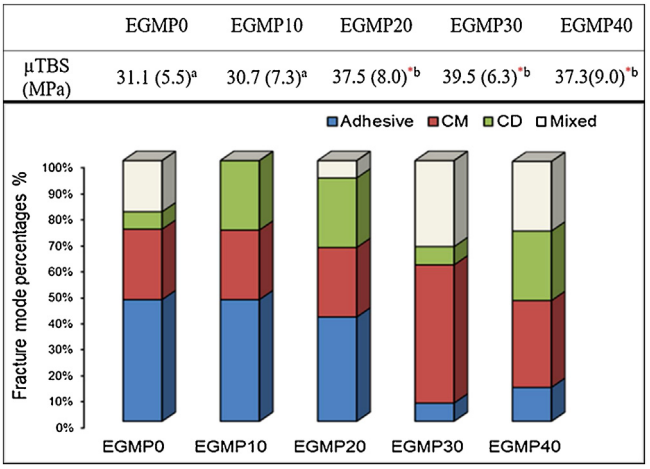

Fig. 4 – Mean microtensile bond strength (μTBS) of the experimental pRMGICs and the control. (*) indicate a statistically significant difference of an experimental group from the control ($p < 0.05$), similar letters indicate no statistically significant differences between groups. Mode of failure of the experimental pRMGIC bonded to sound dentine after two weeks storage in SBF at 37 °C is shown graphically.

(3.3–2.2 μg/mm³) were below the maximum recommended by the ISO 4049 (7.5 μg/mm³). The early stages of water uptake behaviour was used to calculate diffusion coefficients. The diffusion coefficient decreased with increasing concentration of EGMP.

3.5. *Fluoride release*

The fluoride release up to 60 days are presented in Fig. 3. Short-term fluoride release was significantly lower for the pRMGIC experimental cements (EGMP10-40) in comparison to the control group ($p < 0.05$). The reduced elution was proportional to the amount of EGMP in the matrix at the early stages. However, these correlations did not exhibit any statistically significant difference ($p > 0.05$) after seven days immersion in distilled water, showing a similar pattern of release up to 60 days.

3.6. *Adhesion to sound dentine*

The results of the microtensile bond strength and mode of failure are summarised in Fig. 4. One-way ANOVA analysis of the data revealed statistically significant differences among the groups ($p < 0.001$). Further analysis using Bonferroni multiple comparison tests ($p < 0.05$) showed that the addition of 2 0–40% by weight of EGMP to the commercial RMGIC significantly ($p < 0.05$) enhanced its adhesion strength to sound dentine after two weeks storage in SBF at 37 °C but this was not evident in EGMP 10 ($p = 1.000$). The bond strength values were comparable between EGMP20, EGMP30, and EGMP40 ($p = 1.000$), Fig. 4 and the interfacial failure analysis revealed higher adhesive failure mode in the control and EGMP10 and 20 (~40%). All groups showed cohesive failure within the cement, but it was higher in EGMP30 and 40. Cohesive failure within dentine was also seen in all groups, but it was higher in EGMP10, 20, and 40. Additionally, mixed failure could be recognized in EGMP30, 40, and the control, Fig. 4.

3.7. *SEM analysis of the failed interfaces*

The scanning electron micrographs of fractured specimens obtained from compression testing are presented in Fig. 5. The pRMGIC cements showed a dense microstructure with smaller pores and with higher EGMP concentration, the pRMGIC's clearly showed evidence of particle like deposits.

The fractured specimens obtained post-biaxial flexural strength tests after interaction with SBF over 4 weeks showed irregular shaped particulate deposits and on EDX analysis as shown in Fig. 6 indicated an increase in the intensity of the phosphate peaks, however with the cement matrix containing calcium, it is difficult to obtain a meaningful Ca/P ratio.

4. Discussion

4.1. *Multi-functional pRMGIC cements*

Innovations in the era of minimally invasive dentistry are directed to the multifunctionality of restorative/reparative dental bio-interactive materials. Resin-modified glass-ionomer cements are a class of material with an inherent ability to bond to tooth tissue and leach therapeutic ions. In this study, RMGICs were intercalated with the monomer EGMP in the presence of the existing HEMA monomer to augment the acid-base reaction and create a network of covalently-linked phosphate groups in GICs to yield a novel photo-polymerisable cement. On contact with the tooth structure, the negatively charged phosphoric acid groups of the methacrylate monomers (EGMP) have the ability to bond to Ca^{2+} ions that are present either in tooth apatite [18] or the alkaline glass, thus simultaneously anchoring to both, creating a bridging, stabilising structure.

The effect on the curing parameters (Table 2), at lower concentrations of EGMP, showed no discernible changes were observed in the working time of the cements, however a significant increase ($p < 0.05$) resulted with the higher concen-

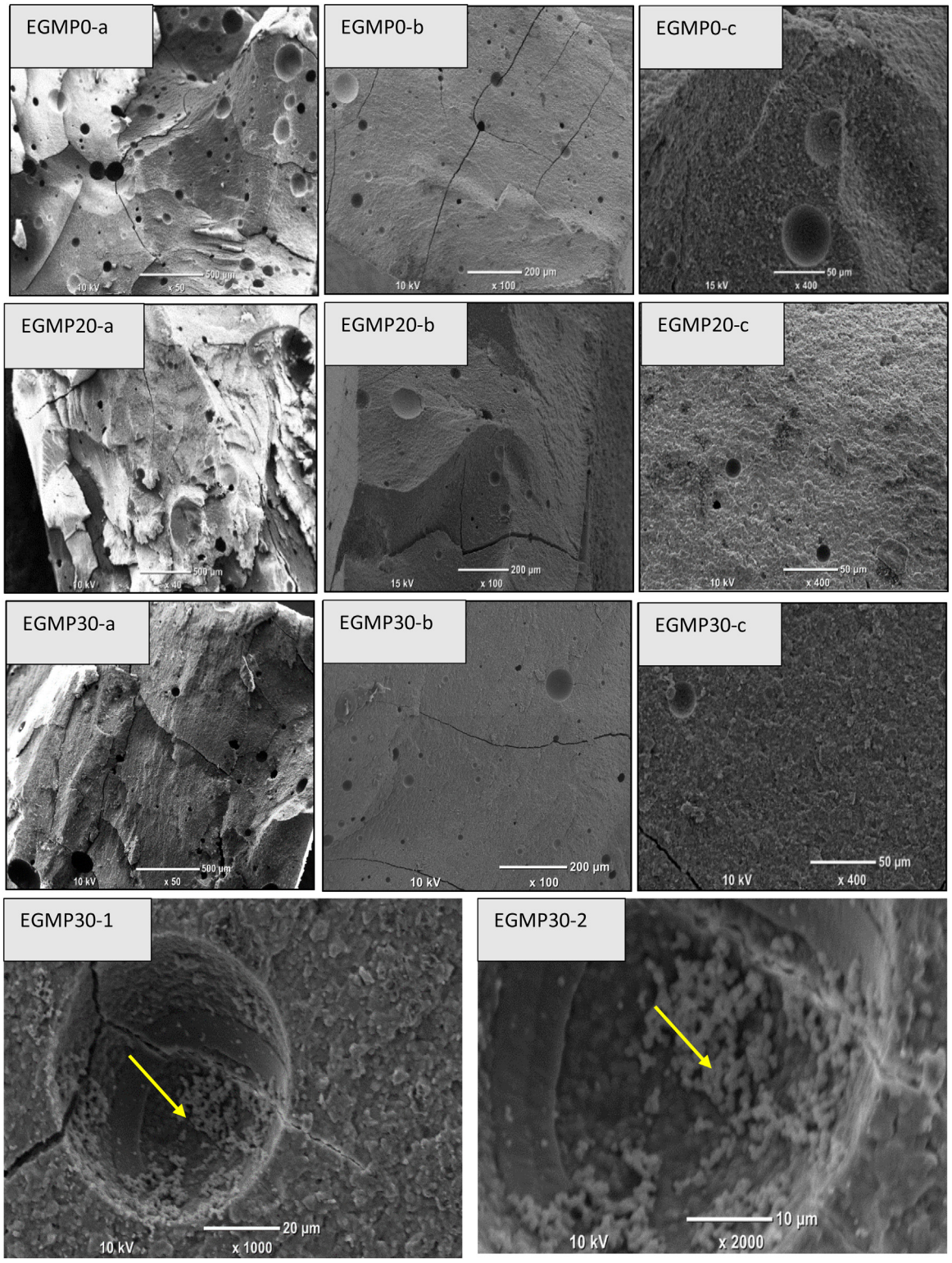

Fig. 5 – Scanning electron micrographs of the fractured compressive test surfaces after 4 weeks immersion in SBF, at ×50, ×100 and ×400 magnification. A more integrated smooth and homogeneous surface with smaller sized pores is observed in EGMP20-c, and 30-c, as compared to that of EGMP0. Yellow arrows in EGMP30-d and e show the presence of a mineral kind of deposit inside the pores of the modified cement (EGMP30) at ×1000, and ×2000 magnification after four weeks ageing in SBF (For interpretation of the references to colour in this figure legend, the reader is referred to the web version of this article).

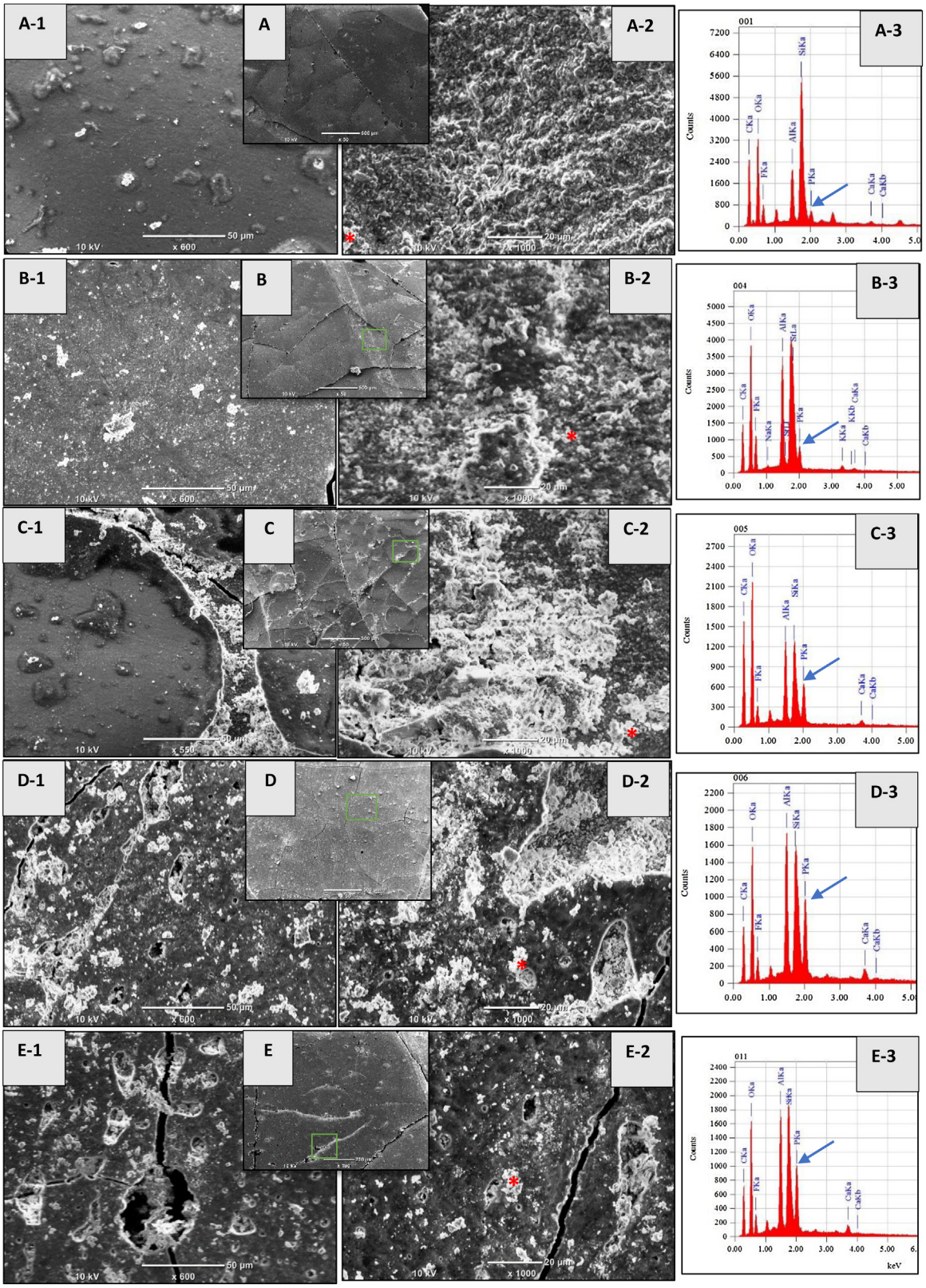

Fig. 6 – SEM-EDX of the fractured surfaces after BFS testing following 4 weeks' immersion in SBF at 37 °C at ×50, ×600 and ×1000 magnification power. Fig. (A–E) represent the surfaces of all groups at ×50 as follow; (A) EGMP0, (B) EGMP10, (C) EGMP20, (D) EGMP30, and (E) EGMP40. These surfaces were further analyzed at higher magnifications (×600, ×1000), Fig. (A–E) (1, 2). Cement matrix in the experimental groups in (B–E) (1, 2) were interspersed by shiny particles irregularly shaped that are not seen in the control group (Fig A-1, 2) that showed no visible changes in the surface morphology after ageing. The red asterisks represent the selected points to be further analyzed by EDX (A–E, 3). The pRMGIC experimental cements

trations of 30–40 wt% EGMP in the formulation. It is interesting to note that at lower concentrations of EGMP, the working time remained unaffected. This was most likely due to the phosphoric acid groups being neutralized and integrated with the calcium ions. The working time of the 30 and 40% EGMP-containing cements was noted to be statistically significantly longer than the control, which may be associated with the competing reaction of the phosphate and carboxyl groups to interact with the calcium ions, nevertheless it still meets the clinical requirements for water-based cements. [19] Importantly, the inclusion of EGMP did not intervene with the setting time of the resultant cements. Since the acid-base reaction occurs due to the presence of the acidic polymer solution and alkaline glass powder irrespective of the presence of EGMP, which undergoes photo-polymerization, the setting reaction remains unaffected. EGMP is miscible and compatible with the co-monomer HEMA [14] and the liquid phase of Fuji II LC, which was confirmed by the lack of any evidence of phase separation. The FTIR spectra of the cements confirmed the setting of the pRMGIC cements [23] and the shoulder peak appearing at 966 cm^{-1} confirms the incorporation of EGMP in the matrix but in addition may be attributed to formation of the mineral crystallites.

The study of the interaction of these class of cements with water is vital since the progression of cement setting and maturation is dependent on moisture that drives the acid-base reaction, gained from the oral environment. The interaction with water was studied in accordance to ISO 4049 [20] with the exception of the desiccation step as recommended for measuring desorption as it would risk the removal of either or both the 'loosely' and 'tightly' bound water in RMGIC's, which is essential for the progression of the acid-base reaction. The modified and control cements exhibited a Fickian behavior in the early stages of water diffusion, which is in agreement with previous findings [24]. The trend in water uptake showed a concomitant increase with increasing EGMP content (Table 4), which is attributed to the water affinity of the polar molecule which parallels earlier reports on the proportional correlation between the equilibrium water content of a HEMA-co-EGMP containing hydrogel and the content of EGMP copolymer [14]. The interaction of RMGIC with moisture is complex and several factors control the rate of water uptake and loss; the density of the polymeric network, the concentration of polar sites available for hydrogen bonding, polymer polarity (water affinity for hydrophilic polar groups in the polymer) and polar interactions within the matrix [24,25]. In the pRMGICs, the polarity and interaction of the acidic functional phosphate group is responsible for the higher water affinity, which contributes to the ongoing acid-base reaction and the formation of stable ionic interactions with time that leads to the formation of a denser matrix with lower porosity and micro-voids, as evidenced by scanning electron micrograph images shown in Fig. 5. Although it is difficult to prevent the formation of artificial cracks within RMGIC's due to the desiccation under vacuum, qualitative assessment of the surface indicated absence of large cracks as in the RMGIC (control cement). This "bushy" matrix imposes a certain resistance to water intrusion, decreasing the rate of water diffusion and significantly reducing the solubility as shown in Table 4. They are both correlated with the proportion of the EGMP monomer within the matrix; the greater weight percentage of the monomer, the lower the diffusion coefficient and solubility. At low concentrations of EGMP in the pRMGIC experimental formulations the distance between the phosphate groups limit the interaction between these groups and these molecules behave as independent hydrophilic monomeric units, however, at higher concentrations, the interaction between the EGMP units itself and with HEMA monomers may lead to H bonding, which influences the crosslinking density. Furthermore, this tightly bonded polyalkenoate matrix restricts the early fluoride elution during the first 48 h, which is proportional to the concentration of the EGMP within the cement matrix, since the release of F- ion is mainly through diffusion from micro-porosities at this stage [26]. However, the migration of the ions with time show that the cements ultimately show similar behavior when there is no replenishment of the fluoride ions (Fig. 3).

4.1.1. *Mechanical properties of the pRMGICs*

Compressive, flexural strength and microhardness properties are not only a reliable method to estimate function and clinical survival probabilities of a new cement over time but also predicated to the internal structural properties of the modified formulations, which directly influence the behaviour of the cement under load. A statistically significant increase ($p < 0.05$) in compressive strength of all the cements were noted after 14 days ageing in simulated body fluid at physiological temperature in comparison to the compressive strength of cements tested at 24 h (Table 3). When a polyalkenoic acid is mixed with the calcium aluminofluorosilicate glass in presence of water, the protons released from the acid cause the hydrolysis of the glass to release Ca^{2+}, Al^{3+}, F^{-} and PO_4^{3-} ions and consequently polyacrylates are formed, and a siliceous layer surrounds the glass particles to inhibit its further degradation. Since the maturation of the cement occurs over time, mechanical properties of GIC's tend to improve with time and this trend is also observed in RMGICs [27]. Further ageing of the cements showed that the compressive strength of the cements with the higher EGMP concentration (30% and 40%) increased significantly as compared to the control ($p < 0.05$). The long-term ageing (6 months) of all modified formulations presented a statistically significant increase from the commercial reference ($p < 0.05$) and their correspondent values after 24 h (Table 3). The compressive modulus of the pRMGICs were significantly higher ($p < 0.05$) than the control at most time

show a similar chemical composition to the control group A-3 which contain elemental peaks of aluminum, silica, fluoride, phosphorus, and calcium, however the peak intensity of P increased proportionally with increasing EGMP monomer within the cement, as shown by blue arrows (For interpretation of the references to colour in this figure legend, the reader is referred to the web version of this article).

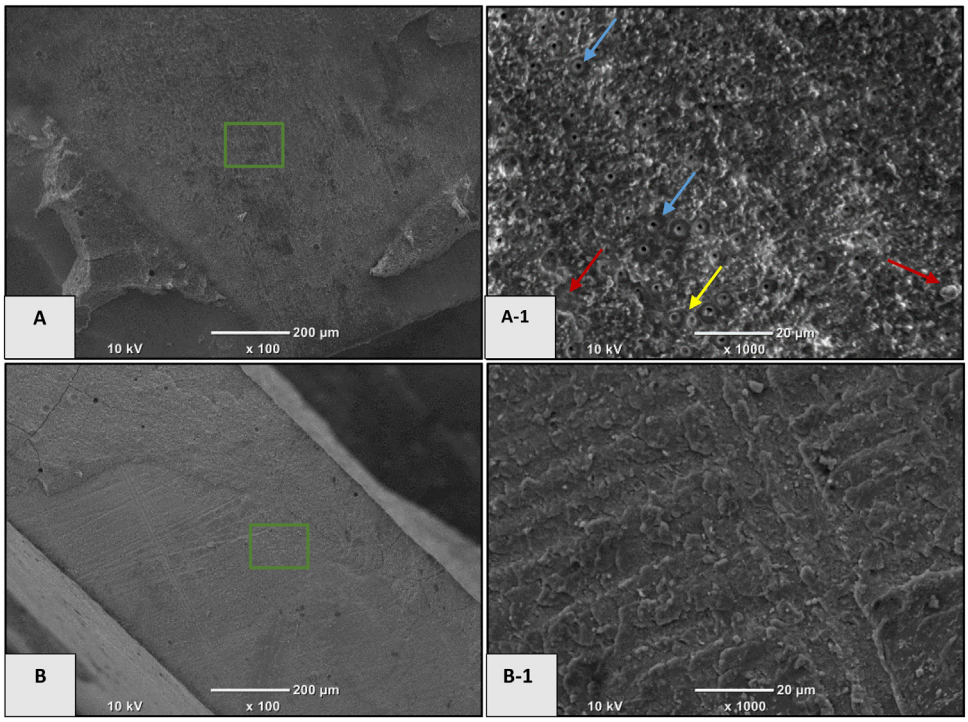

Fig. 7 – Scanning electron micrographs of the debonded interface between Fuji II LC (control) and sound dentin after two weeks storage in SBF at 37 °C. They show mixed failure predominantly adhesive in A, while mostly cohesive in B. The selected areas (green box) showed large number of open dentinal tubules on further magnification (blue arrows) (A-1), with the presence of partially and completely closed tubules (yellow arrow, red arrows, respectively). In Fig. B-1, F2LC is completely covered the debonded area (For interpretation of the references to colour in this figure legend, the reader is referred to the web version of this article).

points and increased proportionally with higher EGMP content within cement matrix. Prolonged ageing of the experimental formulations (EGMP20, 30, and 40) significantly boosted ($p < 0.05$) their compressive modulus values when compared to the control group, and their corresponding values after 24 h, Table 3. The EGMP in the composition of the cement also act as spacer molecules in the polyacid milieu, assisting the movement of the carboxylic acid groups tagged to the rigid polymer backbone providing a greater degree of freedom for the carboxylate ions. This allows higher conversion of the carboxylic acids to metal carboxylate complexes (salt-bridge formation) during the setting reaction and reduces the number of unreacted carboxylic acid groups due to steric hindrance, which in turn improves the strength of the resultant cement [28]. Furthermore, the EGMP monomer with methacrylate residues can be polymerized readily via a free-radical initiation producing a covalently linked matrix of random homopolymers or even copolymerized with HEMA-producing copolymers of EGMP-HEMA [14,29]. Both polymers can reinforce the matrix yielding cements with improved properties. The presence of the ligating phosphate groups in the matrix produces a synergistic effect via the formation of a double-network structure. The reduction of pores result in a denser matrix with improved microhardness and the data shown in Table 3 confirmed that the EGMP 30 and EGMP 40 cements exhibited statistically significantly higher values than the control cement ($p < 0.001$) and this trend was apparent even with low fractions of EGMP when the cements were aged over 4 weeks.

The effect of EGMP on the biaxial flexural strength (BFS) is shown in Table 3, indicated up to a two-fold increase in value ($p < 0.001$) in comparison to the control cements at all time intervals. The interatomic or intermolecular forces within the material have a significant effect on the BFS, and the presence of the strong hydrophilic domains within the cement matrix is likely to inhibit the separation of the planes of atoms within matrix [30], increasing the polar-polar interaction [30,31]. This is confirmed by the fact that an increase in the concentration of EGMP increases BFS values with minimal effect on ageing. The physicochemical interactions may also affect the strength of the cement matrix since there is a possibility of formation of H-bonds due to the presence of hydroxyl, phosphate and carbonyl groups within the matrix, reinforcing the cement. The stronger bonds between the organic and inorganic network of the set cement, lead to superior mechanical properties of final set cement.

The results of the biaxial flexural strength are consistent with the SEM findings that show a denser microstructure of the experimental cements (EGMP20,30) in comparison to the control. The microstructural and surface assessment of the fractured EGMP-contained cement using SEM as shown in Fig. 6 (EGMP30-1 and 2), show dispersion of particles with varying size and shape with clear evidence of mineral deposits at the surface and within matrix pores accompanied by morpholog-

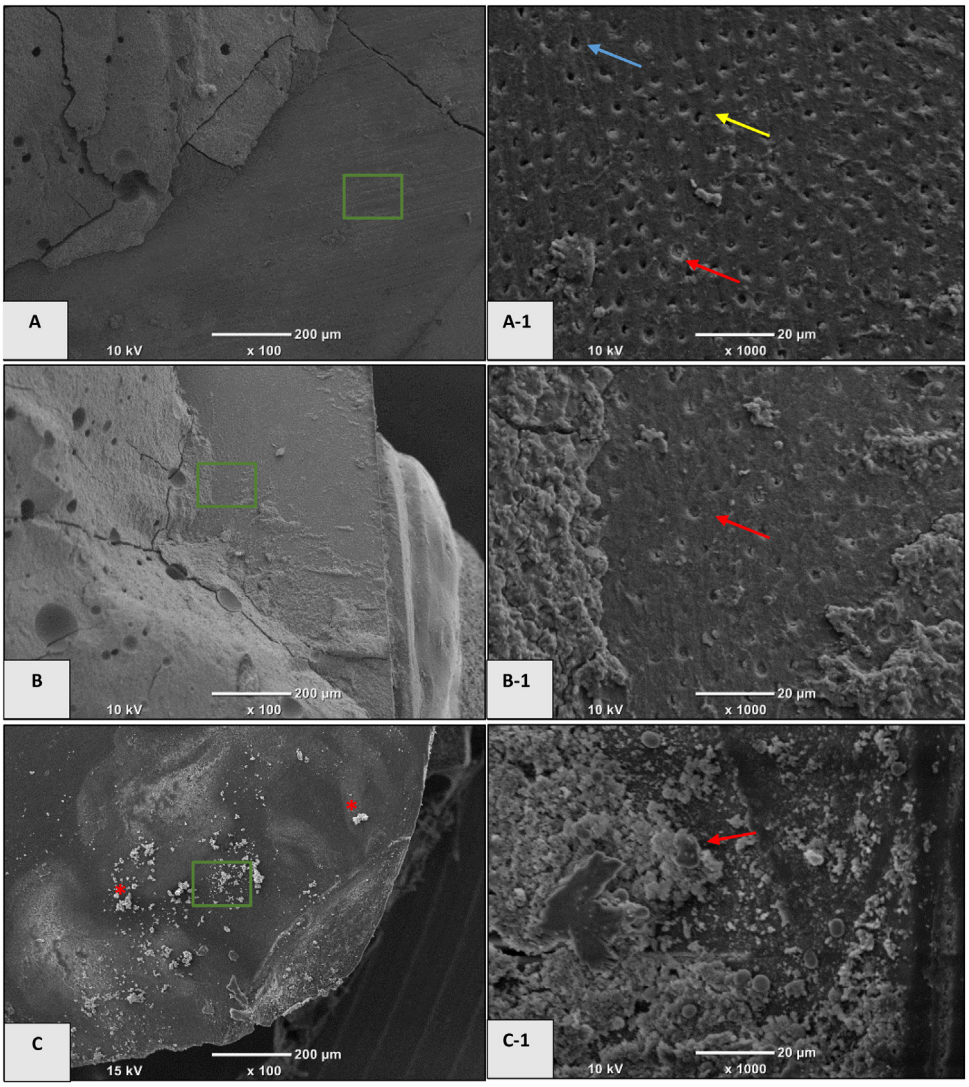

Fig. 8 – Scanning electron micrographs of the debonded interface between EGMP30 and sound dentine after two weeks storage in SBF at 37 °C.They show mixed failure predominantly adhesive in A, mostly cohesive in B, and completely adhesive in C. When a selected area in the green box was further magnified to ×1000 in (A-1), most of the dentinal tubules are recognized as partially or completely closed (yellow, red arrows, respectively) with some of the cement still attached to the surface with the presence of some opened tubules (blue arrows). In B-1, EGMP30 covered the debonded area with completely closed tubules (red arrow). In C there is an evidence of irregular shaped granular patches distributed (red asterisk) over the adhesively debonded cement-dentin interface indicated the mineral forming potential of the cement. On further magnification (C-1), part of the cement was observed to be attached to the dentine surface with complete obliteration of the dentinal tubules (For interpretation of the references to colour in this figure legend, the reader is referred to the web version of this article).

ical surface variations distinctly different from the particles of the cement observed in EGMP0. These changes confirm the inductive ability of these negatively charged functional groups for apatite precipitation within the body environment, similar to findings by Stancu et al. [32]. The FTIR spectra in Fig. 2 supported this evidence, as the modified formulations showed a strong, absorption band at 966 $^{-1}$cm assigned to $\upsilon 1$ stretching vibration of the phosphate PO_4^{3-} in the apatite.

Furthermore, EDX analysis for both experimental and the control cements showed a distribution of the F, Si, Al, P and Ca within their matrices, however, it was difficult to obtain a meaningful Ca:P ratio although an abundance of P was observed within the modified formulations which increased proportionally with the increasing content of the acidic functional monomer within the cement matrix. However, Ca^{2+} ions detected were much lower especially in the pRMGIC's, which is attributed to the reduction in the oxidation state of these calcium atoms due to the charge transfer process, as the calcium acts as an electron acceptor. Calcium atoms that are referred to the RMGIC glass powder are crosslinked by the organic functional groups of the polyacrylic acid and the phosphate-based

monomer as well, which is expected to change their electronic structure [33].

4.1.2. *Interaction of the cements with sound dentine*

RMGIC has a self-etching effect on dentine that augments the hybridisation with dentine, which is reflected in the micro-tensile bond strengths achieved. Since the pRMGIC's contain the additional functional co-monomer EGMP, the lower pH and the chelating ability of the phosphate groups with the residual hydroxyapatite [10] in dentine lead to a more robust and durable bond with dentine over time, thereby accounting for the higher micro-tensile bond strengths reported in this study, Figs. 4 and 7. These interactions are further confirmed by a shift in the mode of failure from predominantly adhesive in the control group to mixed and cohesive patterns for the EGMP30 and 40, Fig. 8. An improved adaptation of the cement to the dentine is most likely caused by the moisture present that is expected to be reused by the reaction between the acidic functional groups and the ion-releasing basic filler particles.

Glass-ionomer and resin-modified glass-ionomer cements can bond chemically to tooth tissue via the formation of an ion-enriched layer by the reaction of the carboxylic acid groups from the polyacid and calcium ions from the tooth tissues. However, they are unable to remineralise apatite-depleted dentine [34]. This is attributed to the lack of nucleation of new apatite even in presence of remineralising analogues and the inhibitory effect of polyacrylic acids on apatite formation. The interaction of EGMP0 versus the EGMP30 with dentine was determined morphologically using scanning electron micrograph in Figs. 7, and 8, respectively. Partial and complete closure of the dentine tubules can be observed on the dentine surface with mixed failure as compared to the control group. Additionally, dispersion of irregularly shaped particles could be recognized over the dentine surface following the interfacial adhesive failure of the dentine/EGMP30, as shown in Figure 12 (C, and C-1). This is indicative of mineral deposition over the surface after two weeks immersion in SBF at 37 °C, which indicates a possibility of the new cement (pRMGIC) being able to induce mineralization when placed over a sound dentine substrate. However, as alluded earlier, it is difficult to analyze the deposits by EDX-SEM, and further studies are required for confirmation.

5. Conclusions

The novel pRMGI cements with a polymerisable phosphate containing co-monomers yielded superior physical properties and exhibited the ability to decalcify tooth apatite with simultaneous chemical bonding thereby enhancing the cement-tooth interfacial interaction. The potential of these cements by virtue of the pendant phosphate groups of the polymeric matrix to remineralise hybrid layers and restore mineral depleted dental collagen structures makes this a unique class of cements. The null hypotheses were rejected.

Acknowledgements

The authors would like to thank GC Corp, Europe for providing the materials for this study. The author Lamis Al-Taee acknowledges the scholarship support from the University of Baghdad, Ministry of Higher Education and Scientific Research, Iraq.

REFERENCES

[1] Selwitz RH, Isamail AI, Pitts NB. Dental caries. Lancet 2007;369:51–9.
[2] Costa Simone M, Martins Carolina C, Bonfim Maria de Lourdes C, Zina Lívia G, Paiva Saul M, Pordeus Isabela A, et al. A systematic review of socio economic indicators and dental caries in adults. Int J Environ Res Public Health 2012;9(10):3540–74.
[3] Marcenes W, Kassebaum NJ, Bernabe E, Flaxman A, Naghavi M, Lopez A, et al. Global burden of oral conditions in 1990–2010: a systematic analysis. J Dent Res 2013;92(7):592–7.
[4] Petersen PE, Bourgeois D, Ogawa H, Estupinan-Day S, Ndiaye C. The global burden of oral disease and risks to oral health. Bull World Health Organ 2005;83(9):661–9.
[5] Green D, Mackenzie L, Banerjee A. Minimally invasive long-term management of direct restorations: the '5 Rs'. Dent Update 2015;42(5):413–6.
[6] Dobloug A, Grytten J. Dentist-specific effects on the longevity of dental restorations. Community Dent Oral Epidemiol 2015;43:68–74.
[7] Mjör IA, Gordan VV. Failure, repair, refurbishing and longevity of restorations. Oper Dent 2002;27:528–34.
[8] Hickel R, Manhart J. Longevity of restorations in posterior teeth and reasons for failure. J Adhes Dent 2001;3:45–64.
[9] Kanzow P, Hoffmann R, Tschammler C, Kruppa J, Rödig T, Wiegand A. Attitudes, practice, and experience of German dentists regarding repair restorations. Clin Oral Investig 2017;21:1087–93.
[10] Blum IR, Lynch CD, Wilson NF. Factors influencing repair of dental restorations with resin composite. Clin Cosmet Investig Dent 2014;6:81–7.
[11] Eltahlah D, Lynch CD, Chadwick BL, Blum IR, Nairn H, Wilson F. An update on the reasons for placement and replacement of direct restorations. J Dent 2018;72:1–7.
[12] Nicholson J, Czarnecka B. Materials for the direct restoration of teeth. UK: Woodhead Publishing; 2016. p. 137.
[13] Nicholson JW. Adhesion of glass-ionomer cements to teeth: A review. Int J Adhes 2016;69:33–8.
[14] Kemal E, Adesanya KO, Deb S. Phosphate based 2-hydroxyethyl methacrylate hydrogels for biomedical applications. J Mater Chem 2011;21:2237–45.
[15] Inoue S, Koshiro K, Yoshida Y, De Munck J, Nagakane K, Suzuki K, et al. Hydrolytic stability of self-etch adhesives bonded to dentin. J Dent Res 2005;84:1160–4.
[16] Perdigão J, Swift Jr EJ. Universal adhesives. J Esthet Restor Dent 2015;27:331–4.
[17] Van Meerbeek B, Yoshihara K, Yoshida Y, Mine AJ, De Munck J, Van Landuyt KL. State of the art of self-etch adhesives. Dent Mater 2011;27:17–28.
[18] Yoshida Y, Van Meerbeek B, Nakayama Y, Snauwaert J, Hellemans L, Lambrechts P, et al. Evidence of chemical bonding at biomaterial-hard tissue interfaces. J Dent Res 2000;79:709–14.
[19] ISO Specification 9917-2. Standard specification for water-based cements — part 2: resin-modified cements; 2010.
[20] ISO Specification 4049. Standard specification for polymer-based restorative materials; 2009.
[21] Shetty DK, Rosenfield AR, Duckworth WH, Held PR. A biaxial-flexure test for evaluating ceramic strengths. J Am Ceram Soc 1983;66:36–42.

[22] Zankuli MA, Devlin H, Silikas N. Water sorption and solubility of core build-up materials. Dent Mater 2014;30:e324–9.
[23] Young AM. FTIR investigation of polymerization and polyacid neutralization kinetics in resin-modified glass-ionomer dental cements. Biomaterials 2002;23:3289–95.
[24] Kanchanavasita W, Anstice HM, Pearson GJ. Water sorption characteristics of resin-modified glass-ionomer cements. Biomaterials 1997;18:343–9.
[25] Zankuli M, Devlin H, Silikas N. Water sorption and solubility of core build-up materials. Dent Mater 2014;30:324.
[26] Thanjal NK, Billington RW, Shahid S, Luo J, Hill RG, Pearson GJ. Kinetics of fluoride ion release from dental restorative glass ionomer cements: the influence of ultrasound, radiant heat and glass composition. J Mater Sci Mater Med 2010;21:589–95.
[27] Sidhu SK, Nicholson JW. A review of glass-ionomer cements for clinical dentistry. J Funct Biomater 2016;7(3):e16.
[28] Culbertson BM. New polymeric materials for use in glass-ionomer cements. J Dent 2006;34:556–65.
[29] Nuttelman CR, Benoit DS, Tripodi MC, Anseth KS. The effect of ethylene glycol methacrylate phosphate in PEG hydrogels on mineralization and viability of encapsulated hMSCs. Biomaterials 2006;27:1377–86.
[30] Yamazaki T, Brantley W, Culbertson B, Seghi R, Schricker S. The measure of wear in N-vinyl pyrrolidinone (NVP) modifed glassionomer cements. Polym Adv Technol 2005;16:113–6.
[31] Xie D, Wu W, Puckett A, Farmer B, Mays JW. Novel resin modified glass-ionomer cements with improved flexural strength and ease of handling. Eur Polym J 2004;40:343–51.
[32] Stancu IC, Filmon R, Cincu C, Marculescu B, Zaharia C, Tourmen Y, et al. Synthesis of methacryloyloxyethyl phosphate copolymers and in vitro calcification capacity. Biomaterials 2004;25:205–13.
[33] Gerth HU, Dammaschke T, Züchner H, Schäfer E. Chemical analysis and bonding reaction of RelyX Unicem and Bifix composites—a comparative study. Dent Mater 2006;22:934–41.
[34] Kim YK, Yiu CK, Kim JR, Gu L, Kim SK, Weller RN, et al. Failure of a glass ionomer to remineralize apatite-depleted dentin. J Dent Res 2010;89:230–5.